Supporting information

Multivariate Covalent Organic Frameworks Boosting Photocatalytic Hydrogen Evolution

*Ting Zhou, Xingye Huang, Zhen Mi, Yunyang Zhu, Rong Wang, Changchun Wang, and Jia Guo**

State Key Laboratory of Molecular Engineering of Polymers, Department of Macromolecular Science, Fudan University, Shanghai 200433, China.

*E-mail: guojia@fudan.edu.cn

Section I. Materials and Characterizations

1. Materials

Anhydrous 1,2-dichlorobenzene, anhydrous n-butanol, and chloroplatinic acid hexahydrate were purchased from Aladdin Industrial Corporation. Tetrahydrofuran (THF), methyl alcohol (MeOH) and acetone were purchased from Shanghai Chemical Regents Company. Ascorbic acid were purchased from Sinopharm Chemical Reagent Co. Ltd.1,3,5-triformylphloroglucinol, 4,4'-(benzo-2,1,3-thiadiazole-4,7-diyl)dianiline and 4,4'-diamino-p-terphenyl were purchased from Jilin Chinese Academy of Sciences-Yanshen technology Co. Ltd. All the chemical materials were used without further purification.

2. Characterizations

Powder X-ray diffraction (PXRD) patterns were collected at room temperature on an X-ray diffraction spectrometer (Bruker D8 Advance, Germany) with Cu Kα radiation at $\lambda = 0.154$ nm operating at 40 kV and 40 mA. Fourier transform infrared (FT-IR) spectra were recorded on Nicolet 6700 (Thermofsher, USA) Fourier transformation infrared spectrometer. Diffuse reflectance UV-visible absorption spectra were collected on a Lambda 750 spectrometer (referenced to barium sulphate). Elemental analysis (EA) measurements were analyzed using a vario EL Elemental Analyzer. Inductively coupled plasma atomic emission spectroscopy (ICP-AES) was done on a VARIAN VISTA RL simultaneous spectrometer (Agilent Technologies, Santa Clara, California, USA) with a CCD-detector. High-resolution transmission electron microscopy images were obtained using a JEOL 2100F microscope operated at 200 kV accelerating voltage. The elemental mappings of C, N, O and S atoms were collected using the same transmission electron microscope (operating at 200 kV) under the ADF STEM mode. N_2 adsorption-desorption isotherms were collected by a TriStar II 3020 volumetric adsorption analyzer (Micromeritics, USA) at 77 K. The samples were degassed at 120 °C for 12 h under vacuum before measurement. The surface areas were evaluated using the Brunauer-Emmett-Teller (BET) model applied between P/P0 values of 0.05 and 0.1 for mesoporous COFs. Solid-state CP/MAS ^{13}C NMR spectra were recorded on 400WB AVANCE III (Bruker, Switzerland) plus 400 MHz spectrophotometer at 298 K.

3. Methods

3.1 The AQE measurement

The apparent quantum efficiency (AQE) was measured under the irraidation of a 300 W Xe lamp with different bandpass filters (including 420, 500, 550 and 600 nm) using the following equation:

$$\begin{aligned}\text{AQE}(\%) &= \frac{\text{Number of reacted electrons}}{\text{Number of incident electrons}} \times 100\% \\ &= \frac{2 \times \text{Number of evolved } H_2 \text{ molecules}}{\text{Number of incident photons}} \times 100\%\end{aligned}$$

3.2 Photoelectrochemical measurements

The photocurrent-time (I-t) profiles, electrochemical impedance spectra (EIS), Mott-Schottky plot were recorded on the CHI760E electrochemical workstation with a standard three-electrode system with the photocatalyst-coated ITO as the working electrode, Pt plate as the counter electrode and the Ag/AgCl electrode as a reference electrode. A 0.2 M Na_2SO_4 solution (pH = 6.8) was used as the electrolyte and purged with argon for 30 min prior to the measurement. A 300 W Xenon lamp with a 420 nm cut-off filter was used as the light source during the measurement. The applied potentials vs. Ag/AgCl is converted to RHE potentials using the following equation:

$$E_{RHE} = E_{Ag/AgCl} + 0.0591\text{pH} + E^{\theta}_{Ag/AgCl} \ (E^{\theta}_{Ag/AgCl} = 0.199 \text{ V})$$

3.3 Steady-state photoluminescent emission spectra

Steady-state PL emission spectra were obtained at 298 K with an excitation wavelength of 400 nm. Before measurement, BT-containing monomers were dispersed in a mixture of THF and water with different volume percentages and the concentration was kept at 76.5 μmol L^{-1}.

Section II. Supplementary Figures and Tables

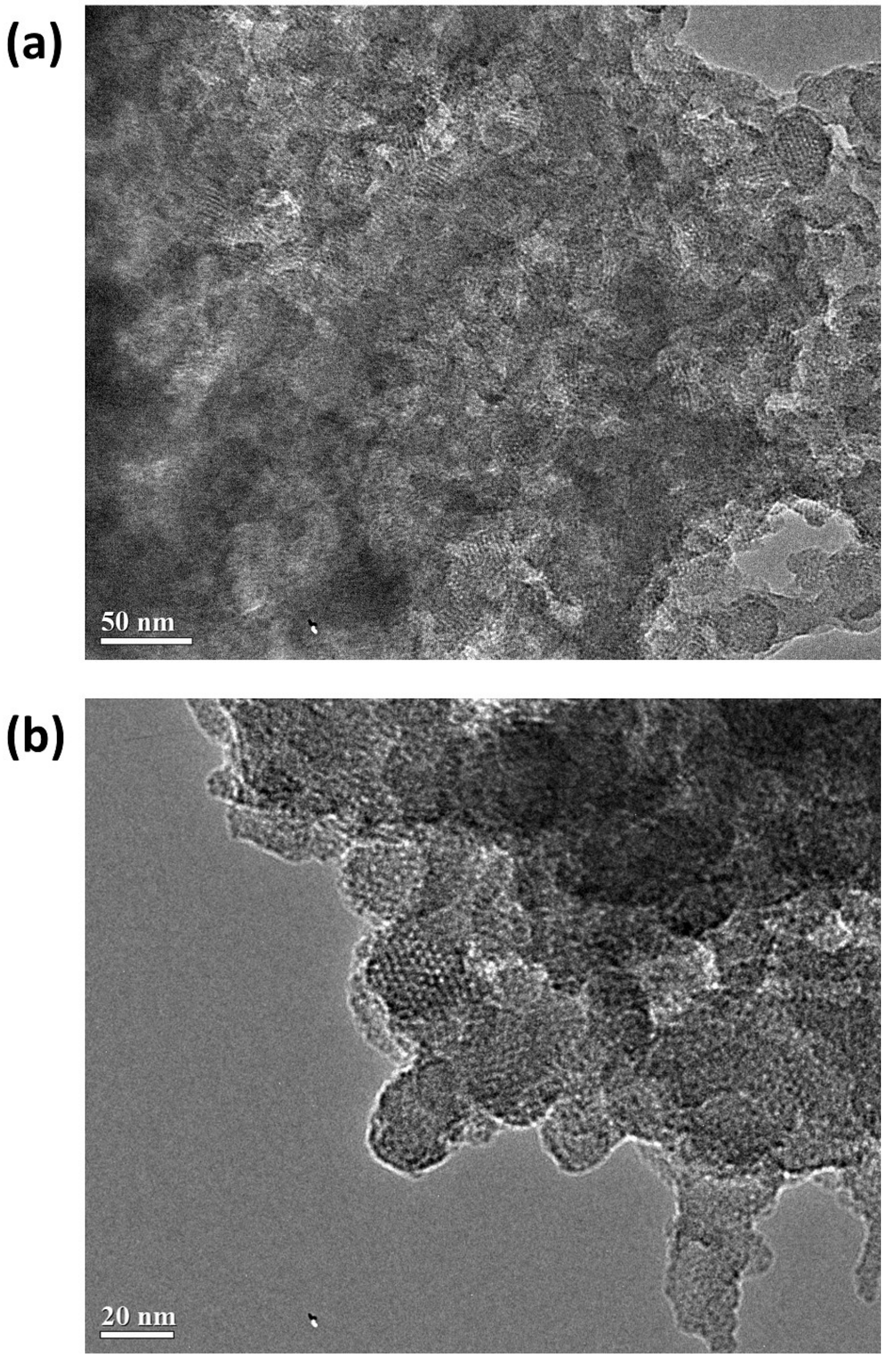

Figure S1. HRTEM images of Tp($BT_{0.05}TP_{0.95}$)-COF.

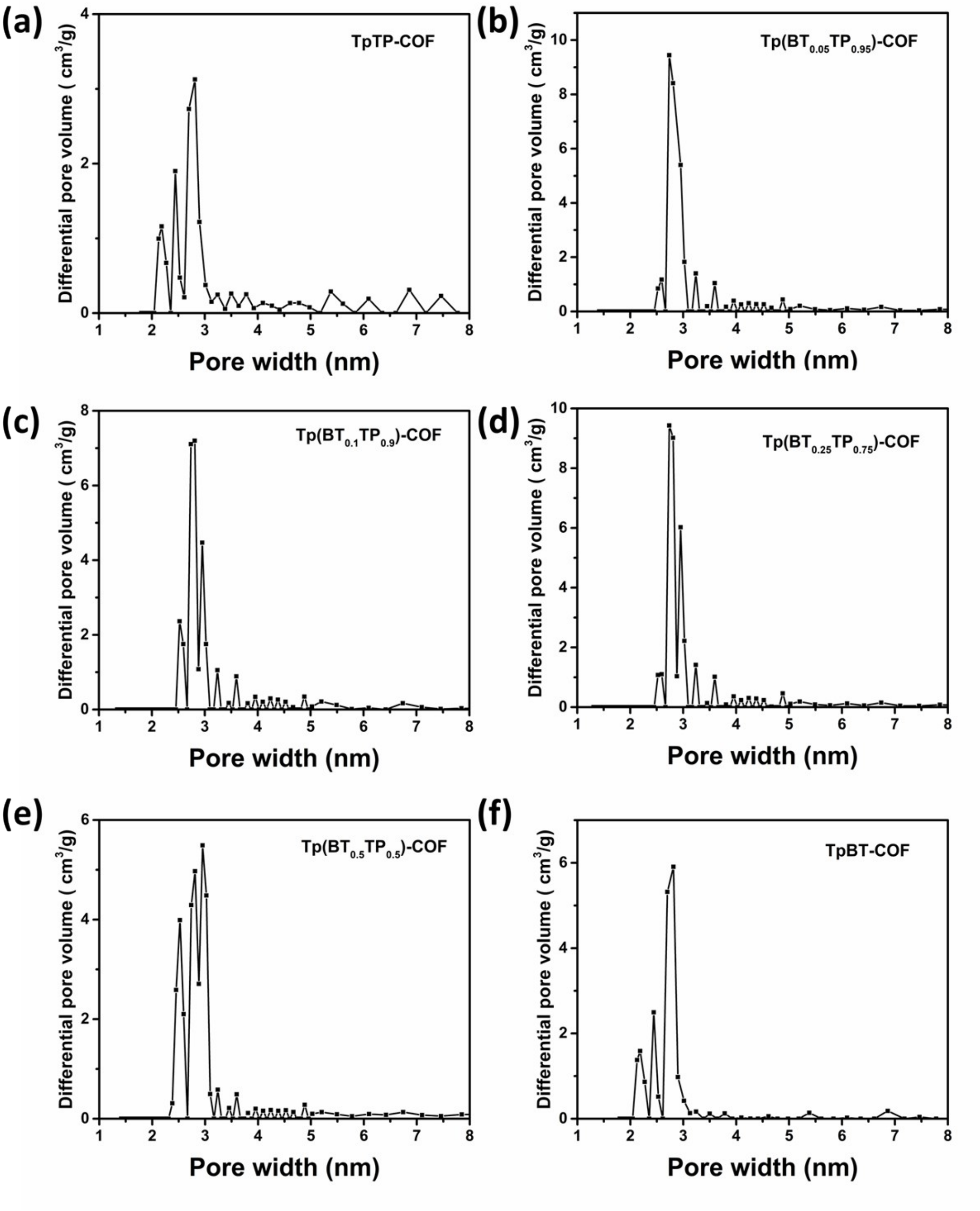

Figure S2. Pore-size distributions of Tp(BT_xTP_{1-x})-COF.

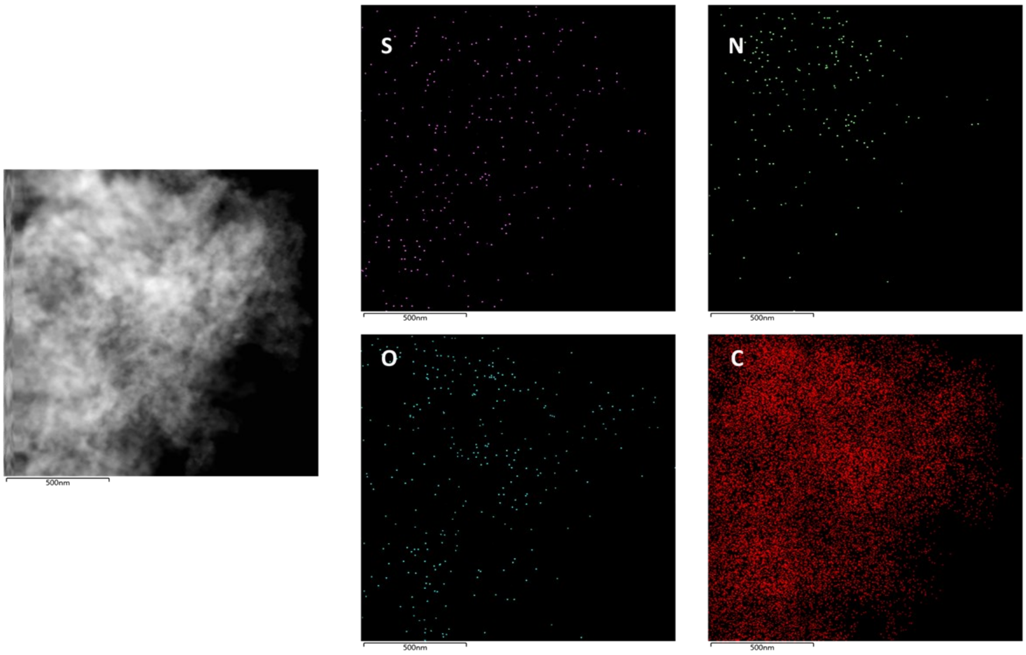

Figure S3. HRTEM image of the Tp($BT_{0.05}TP_{0.95}$)-COF and its corresponding elemental mappings of S (purple), N (green), O (blue) and C (red) atoms.

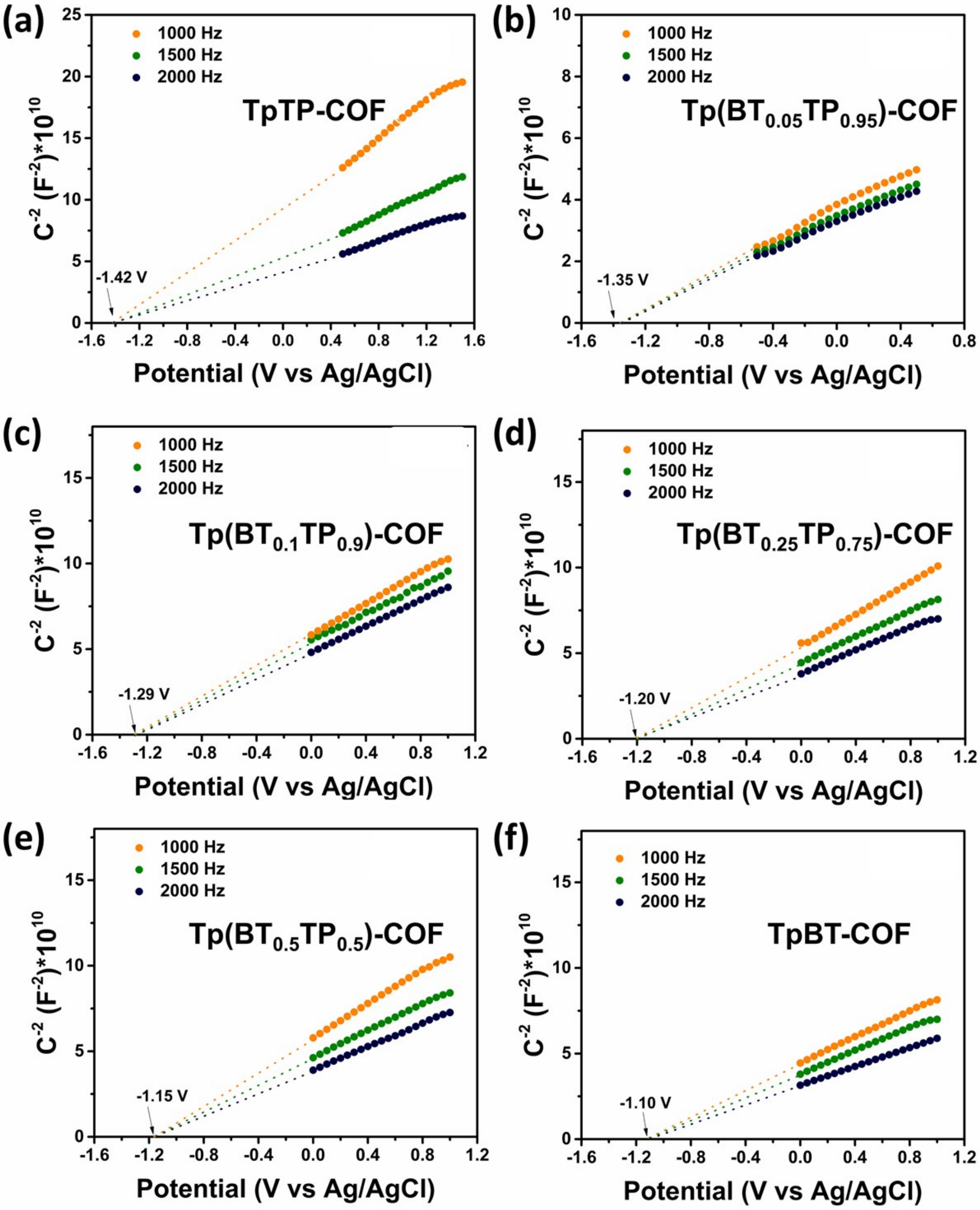

Figure S4. Mott–Schottky plots of TpTP-COF (a), Tp($BT_{0.05}TP_{0.95}$)-COF (b), Tp($BT_{0.1}TP_{0.9}$)-COF (c), Tp($BT_{0.25}TP_{0.75}$)-COF (d), Tp($BT_{0.5}TP_{0.5}$)-COF (e) and TpBT-COF (f).

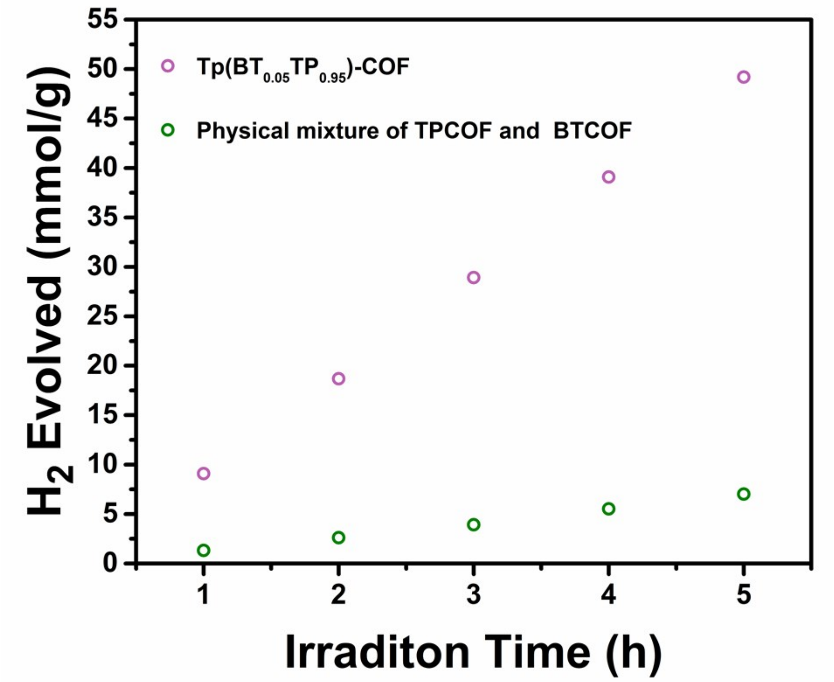

Figure S5. Time course of H_2 evolution using Tp($BT_{0.05}TP_{0.95}$)-COF and the mixture of TpTP-COF and the TpBT-COF added according to the molar ratio of BT and TP in the Tp($BT_{0.05}TP_{0.95}$)-COF, respectively.

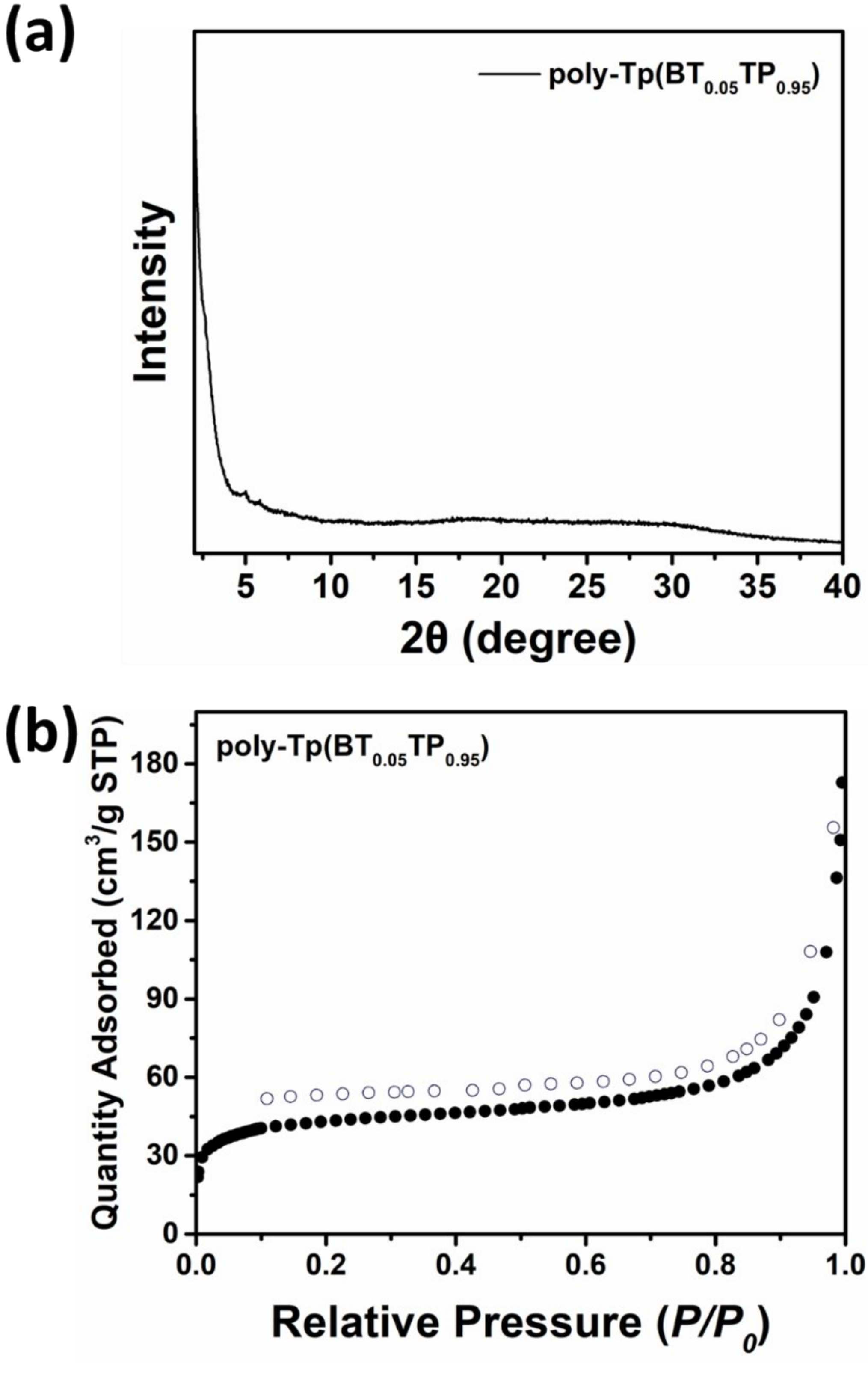

Figure S6. PXRD pattern (a) and N_2 sorption isotherms (b) of the amorphous poly-Tp($BT_{0.05}TP_{0.95}$).

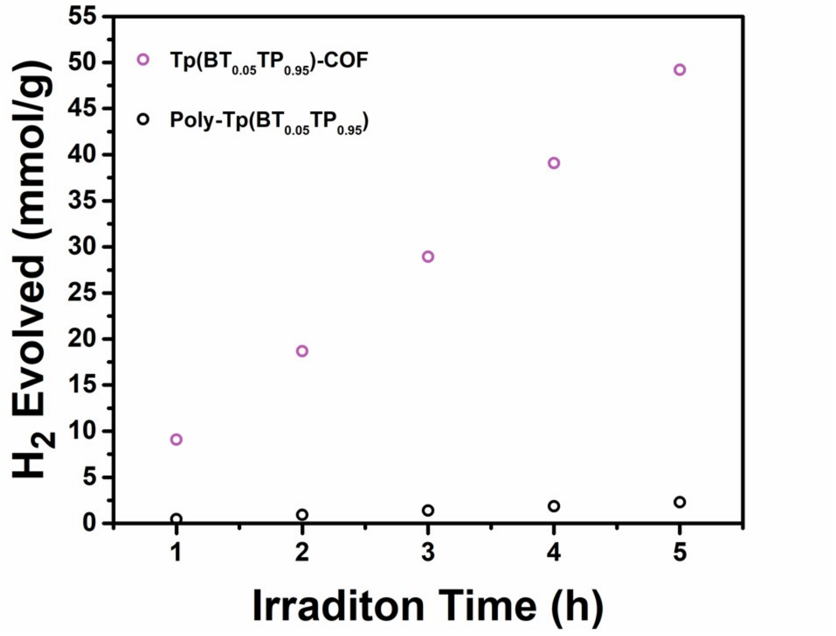

Figure S7. Time course of H_2 evolution using poly-$Tp(BT_{0.05}TP_{0.95})$ as the catalyst.

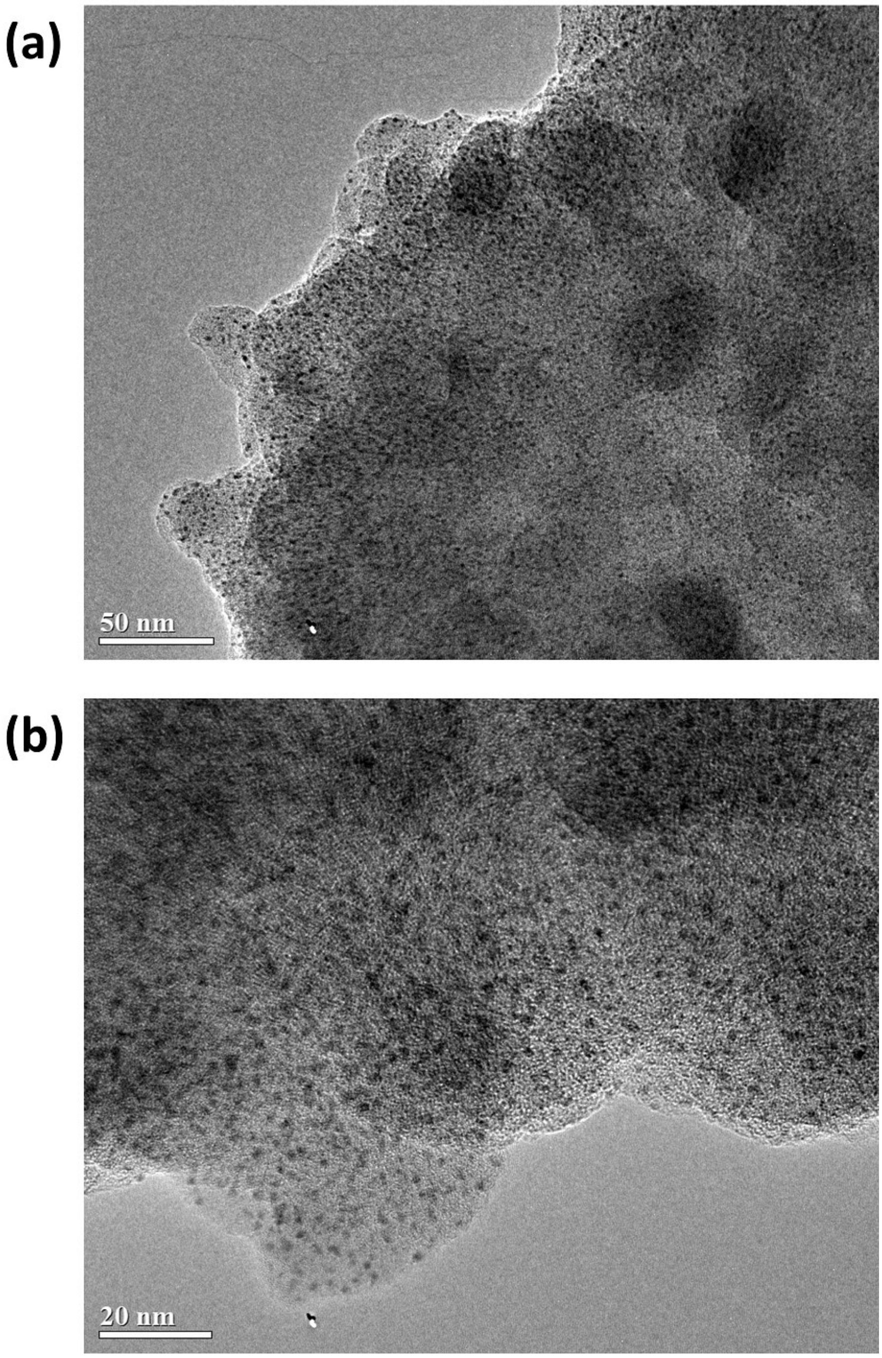

Figure S8. HRTEM images of $Tp(BT_{0.05}TP_{0.95})$-COF after the 30-h photocatalytic test.

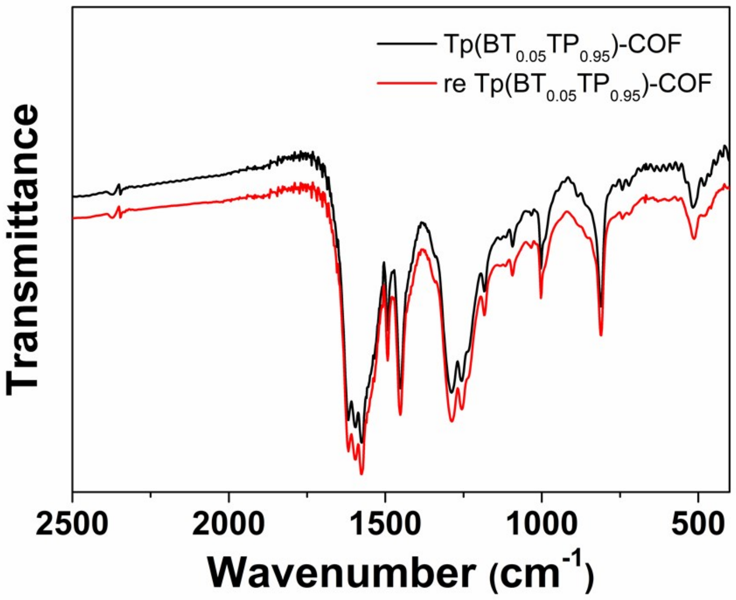

Figure S9. FT-IR spectra of Tp($BT_{0.05}TP_{0.95}$)-COF before (black) and after (red) the 30-h photocatalytic test. The characterization was performed after 30-h H_2 evolution experiment under visible light ($\lambda > 420$ nm).

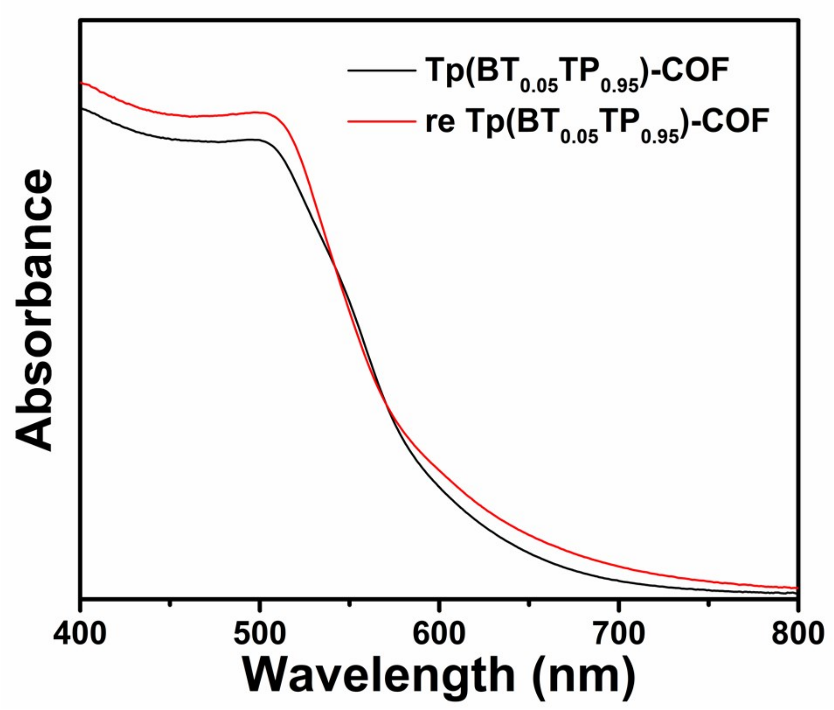

Figure S10. UV-vis diffuse reflectance spectra of the Tp($BT_{0.05}TP_{0.95}$)-COF before (black) and after (red) the 30-h photocatalytic test.

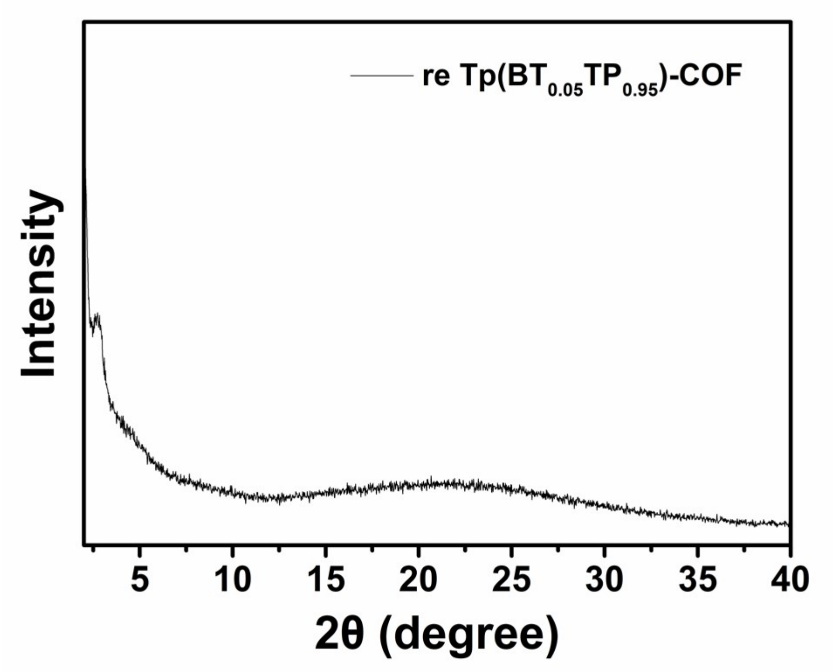

Figure S11. PXRD patterns of the Tp($BT_{0.05}TP_{0.95}$)-COF after the 30-h photocatalytic test.

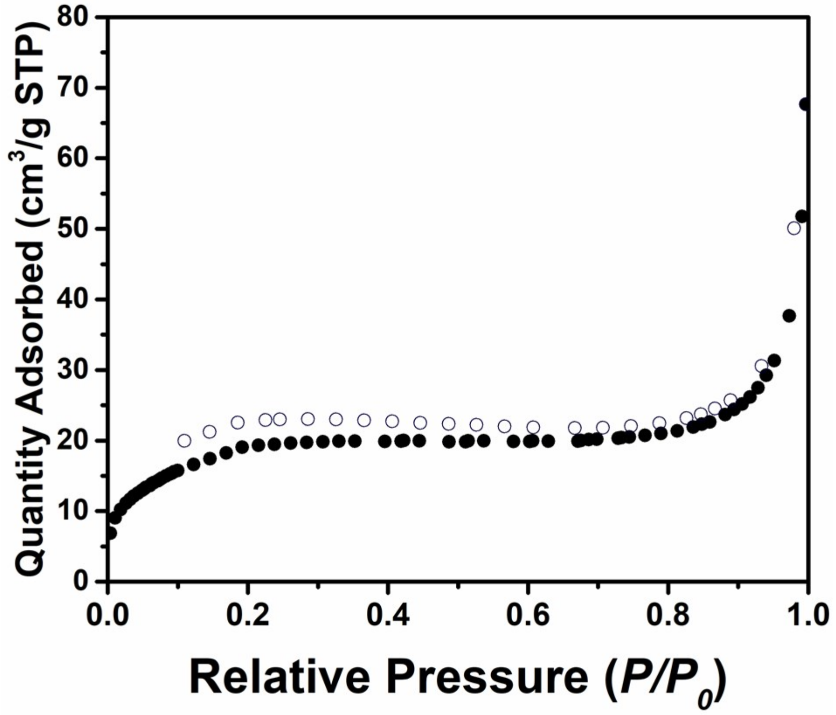

Figure S12. N_2 sorption isotherms of the Tp($BT_{0.05}TP_{0.95}$)-COF after the 30-h photocatalytic test.

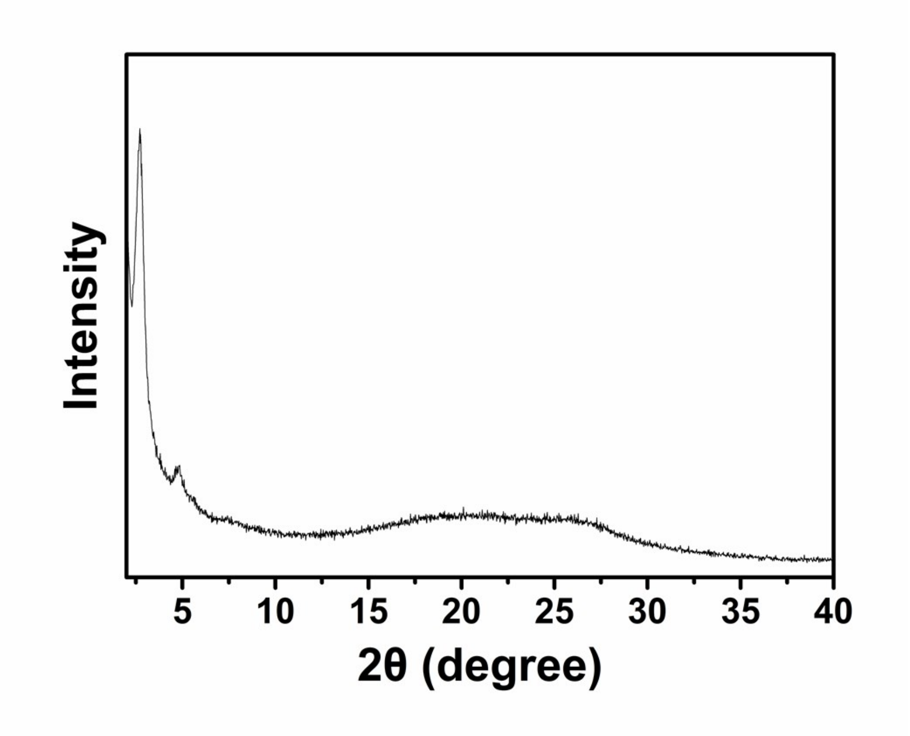

Figure S13. PXRD patterns of the regenerated Tp($BT_{0.05}TP_{0.95}$)-COF by subjecting the powder after photocatalysis into the initial synthetic conditions.

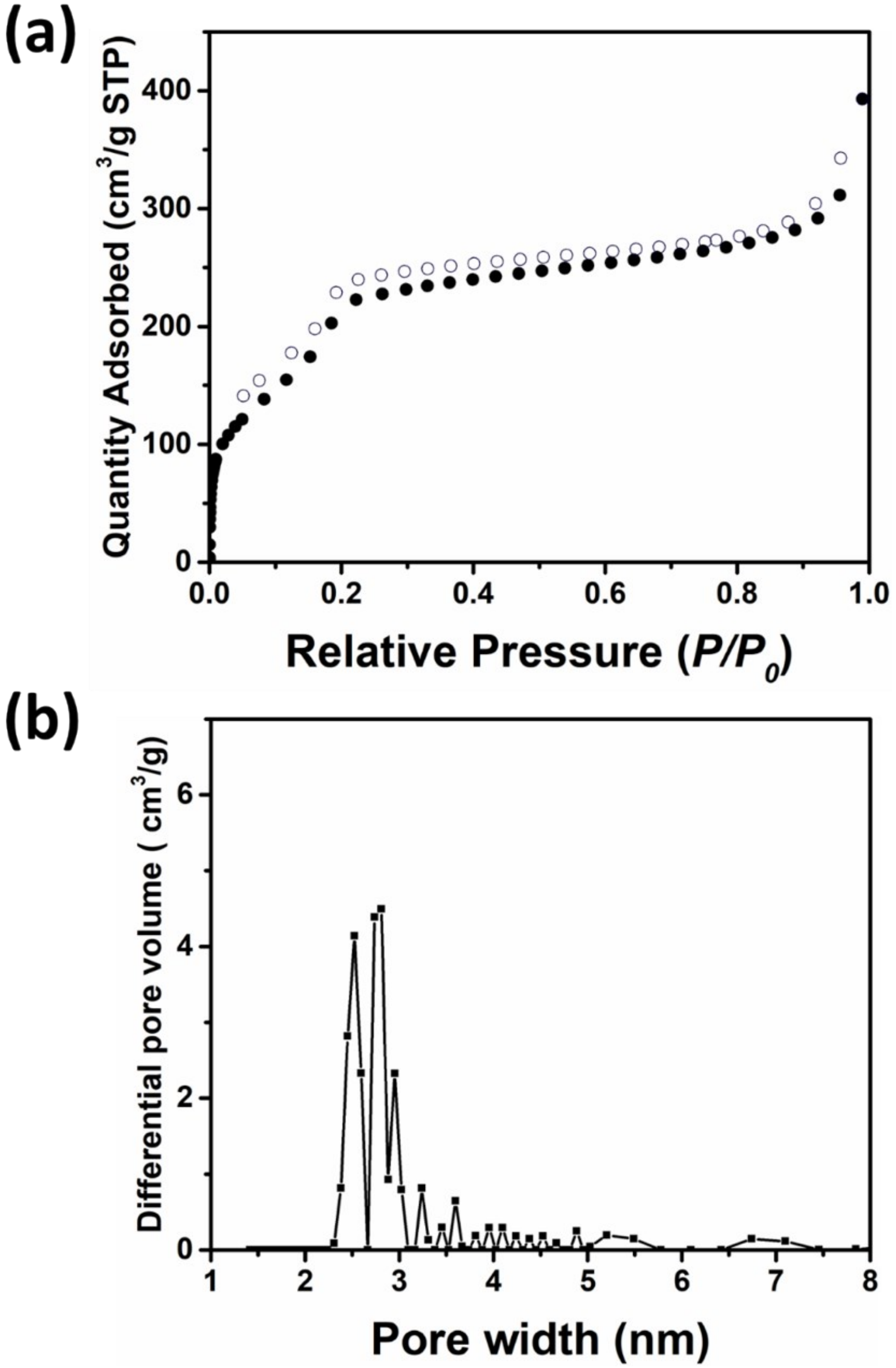

Figure S14. N_2 sorption isotherms (a) and pore-size distributions (b) of the regenerated Tp($BT_{0.05}TP_{0.95}$)-COF, respectively.

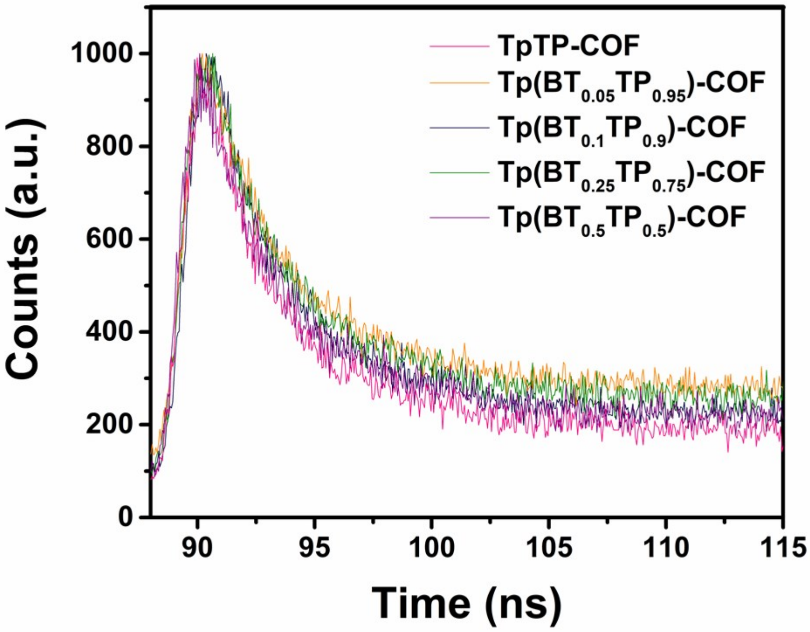

Figure S15. TCSPC measured fluorescence decay profiles of samples.

Table S1. Element Analysis results of the samples.

Sample	C(wt%)		H(wt%)		N(wt%)		S(wt%)	
	Found	**Cal.**	**Found**	**Cal.**	**Found**	**Cal.**	**Found**	**Cal.**
TpTP-COF	78.56	79.09	5.39	5.53	8.22	7.69	-	0.00
Tp($BT_{0.05}TP_{0.95}$)-COF	78.02	78.47	5.35	5.46	8.60	8.01	0.39	0.44
Tp($BT_{0.1}TP_{0.9}$)-COF	77.43	77.86	5.22	5.39	8.76	8.32	0.79	0.86
Tp($BT_{0.25}TP_{0.75}$)-COF	76.04	76.07	5.19	5.18	9.75	9.24	1.91	2.11
Tp($BT_{0.5}TP_{0.5}$)-COF	72.89	73.26	4.65	4.87	11.07	10.68	3.82	4.08
TpBT-COF	67.82	68.23	4.04	4.29	13.61	13.26	7.61	7.59

Table S2. Pt contents of the different samples measured by ICP-AES.

	Feeding content (*wt.*%)	ICP content (*wt.*%)
TpTP-COF	5	3.37
Tp($BT_{0.05}TP_{0.95}$)-COF	5	3.43
Tp($BT_{0.1}TP_{0.9}$)-COF	5	3.39
Tp($BT_{0.25}TP_{0.75}$)-COF	5	3.49
Tp($BT_{0.5}TP_{0.5}$)-COF	5	3.51
TpBT-COF	5	3.46

Table S3. Photocatalytic hydrogen evolution performances of the different COF-based photocatalysts.

Photocatalyst	**Co-catalyst**	**SED**	**Illumination**	**HER (mmol g^{-1} h^{-1})**	**AQE**	**Ref.**
TFPT-COF	3% Pt	10 vol% TEOA	> 420nm	1.97	2.2-3.9% at 500nm	[S1]
N$_3$-COF	3% Pt	1 vol% TEOA pH = 7	> 420nm	1.703	0.44% at 450nm	[S2]
PTP-COF	3% Pt	1 vol% TEOA pH = 7	AM1.5	0.084		[S3]
TP- BDDA-COF	3% Pt	10 vol% TEOA	> 395 nm	0.33	1.3% at 420 nm	[S4]
FS-COF	8% Pt	0.1 M ascorbic acid	> 420 nm	10.1	3.2% at 420 nm	[S5]
S-COF	8% Pt	0.1 M ascorbic acid	> 420 nm	4.44		[S5]
A-TEBPY-COF	3% Pt	10 vol% TEOA pH = 7	AM1.5	0.098		[S6]
CTF-HUST-C1	3% Pt	10 vol% TEOA	> 420 nm	5.1		[S7]
SP^2-COF$_{ERDN}$	3% Pt	10 vol% TEOA	> 420 nm	2.12	0.47% at 520 nm	[S8]
g-C$_{40}$N$_3$-COF	3% Pt	10 vol% TEOA	> 420 nm	4.12	4.84% at 420 nm	[S9]
TP-COF	6% PVP-Pt	0.054 M ascorbic acid	> 420 nm	8.42	0.4% at 420 nm	[S10]
CTF-HUST-A1-^{t}BuOK	3% Pt	10 vol% TEOA	> 420 nm	9.2	7.4% at 420 nm	[S11]
Py-ClTP-BT-COF	Pt	0.1 M ascorbic acid	> 420 nm	8.88	8.45% at 420 nm	[S12]
BtCOF150	1%Pt	20 vol%TEOA pH=11	> 420 nm	0.75	0.2% at 420 nm	[S13]
BtTpCOF	1%Pt	20 vol%TEOA pH=11	> 420 nm	0.45		[S13]
BtAntCOF	1%Pt	20 vol%TEOA pH=11	> 420 nm	0.11		[S13]
NTU-BDA-THTA	Pt	0.1 M ascorbic acid	> 420 nm	1.13		[S14]
Tp(BT$_{0.05}$TP$_{0.95}$)-COF	**3.4% Pt**	**0.1 M ascorbic acid**	**> 420 nm**	**9.84**	**2.34% at 420 nm**	**This work**
Tp(BT$_{0.1}$TP$_{0.9}$)-COF	**3.4%Pt**	**0.1 M ascorbic acid**	**> 420 nm**	**7.40**		**This work**
Tp(BT$_{0.25}$TP$_{0.75}$)-COF	**3.5%Pt**	**0.1 M ascorbic acid**	**> 420 nm**	**5.82**		**This work**
Tp(BT$_{0.5}$TP$_{0.5}$)-COF	**3.5%Pt**	**0.1 M ascorbic acid**	**> 420 nm**	**5.70**		**This work**

Supplementary References

[S1] L. Stegbauer, K. Schwinghammer and B. V. Lotsch. *Chem. Sci.* 2014, **5**, 2789-2793.

[S2] V. S. Vyas, F. Haase, L. Stegbauer, G. Savasci, F. Podjaski, C. Ochsenfeld and B. V. Lotsch. *Nat. Commun.* 2015, **6**, 8508.

[S3] F. Haase, T. Banerjee, G. Savasci, C. Ochsenfeld and B. V. Lotsch. *Faraday Discuss.* 2017, **201**, 247-264.

[S4] P. Pachfule, A. Acharjya, J. Roeser, T. Langenhahn, M. Schwarze, R. Schomaecker, A. Thomas and Schmidt, J. *J. Am. Chem. Soc.* 2018, **140**, 1423–1427.

[S5] X. Wang, L. Chen, S. Y. Chong, M. A. Little, Y. Wu, W. H. Zhu, R. Clowes, Y. Yan, M. A. Zwijnenburg, R. S. Sprick and A. I. Cooper, *Nat. Chem.* 2018, **10**, 1180-1189.

[S6] L. Stegbauer, S. Zech, G. Savasci, T. Banerjee, F. Podjaski, K. Schwinghammer, C. Ochsenfeld and B. V. Lotsch. *Adv. Energy Mater.* 2018, **8**, 1870107.

[S7] M. Liu, Q. Huang, S. Wang, Z. Li, B. Li, S. Jin and B. Tan, *Angew. Chem. Int. Ed.* 2018, **57**, 11968-11972.

[S8] E. Jin, Z. Lan, Q. Jiang, K. Geng, G. Li, X. Wang and D. Jiang, *Chem* 2019, **5**, 1632-1647.

[S9] S. Bi, C. Yang, Q. Zhang, J. Xu, L. Liu, D. Wu, X. W, Y. Han, Q. Liang and F. Zhang, *Nat. Commun.* 2019, **10**, 2467.

[S10] J. Ming, A. Liu, J. Zhao, P. Zhang, H. Huang, H. Lin, Z. Xu, X. Zhang, X. Wang, J. Hofkens, M. B. Roeffaers and J. Long. *Angew. Chem. Int. Ed.* 2019, **58**, 18290-18294.

[S11] S. Zhang, G. Cheng, L. Guo, N. Wang, B. Tan, and S. Jin. *Angew. Chem. Int. Ed.* 2020, **59**, 6007-6014.

[S12] W. Chen, L. Wang, D. Mo, F. He, Z. Wen, X. Wu, H. Xu and L. Chen, *Angew. Chem. Int. Ed.* 2020, **59**, 16902-16909.

[S13] S. Ghosh, A. Nakada, M. A. Springer, T. Kawaguchi, K. Suzuki, H. Kaji, I. Baburin, A. Kuc, T. Heine, H. Suzuki, R. Abe and S. Seki, *J. Am. Chem. Soc*. 2020, **142**, 9752-9762.

[S14] F. Auras, H. Wang, C. Qian, J. Liu, Y. Zeng, D. Wang, W. Zhou, L. Gu, H. Wu, G. Liu, Y. Zhao, J. Am. Chem. Soc. 2020, **142**, 4862.